Supporting Information

Multi-Phase Porous Electrochemical Catalysts Derived from Iron-Based Metal-Organic Framework Compounds

Kai Liu,[†,‡] Menglin Yu,[†] Haiying Wang,[†] Juan Wang,[†] Weiping Liu,[†] Michael R. Hoffmann[‡,*]

[†] College of Environmental and Resource Sciences, Zhejiang University, Hangzhou 310058, China

[‡] Department of Environmental Science and Engineering, California Institute of Technology, Pasadena, California 91126, United States

Summary:

Pages: 16

Tables: 5

Figures: 29

Table S1. Pesticides used in this study.

No.	Pesticide name	IUPAC name	Formula	Structure	CAS
1	Acetochlor	2-Chloro-*N*-(ethoxymethyl)-*N*-(2-ethyl-6-methylphenyl)acetamide	$C_{14}H_{20}ClNO_2$	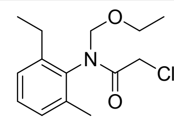	34256-82-1
2	Atrazine	6-chloro-N^2-ethyl-N^4-(propan-2-yl)-1,3,5-triazine-2,4-diamine	$C_8H_{14}ClN_5$	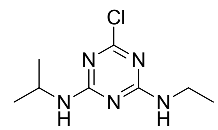	1912-24-9
3	Dichlorprop	(*R*)-2-(2,4-dichlorophenoxy)propanoic acid	$C_9H_8Cl_2O_3$	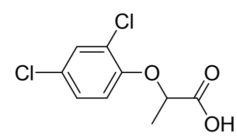	120-36-5
4	Glyphosate	*N*-(phosphonomethyl)glycine	$C_3H_8NO_5P$	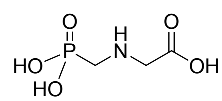	1071-83-6
5	Metolachlor	(*RS*)-2-Chloro-*N*-(2-ethyl-6-methyl-phenyl)-*N*-(1-methoxypropan-2-yl)acetamide	$C_{15}H_{22}ClNO_2$	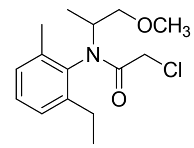	51218-45-2
6	Napropamide	N,N-diethyl-2-(naphthalen-1-yloxy)propanamide	$C_{17}H_{21}NO_2$	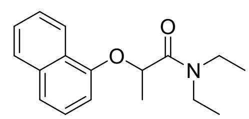	15299-99-7

Table S2. Pseudo-first order rate constant and square regression coefficient for electro-Fenton degradation of napropamide (C_0 = 10 ppm).

Sample name	Reaction conditions		K_{app} (h^{-1})	r^2
	potential (V)	electrolyte pH		
CMIL-88@PCM	-0.345	7	0.99	0.990
CMIL-100@PCM	-0.345	7	1.70	0.997
CMIL-101@PCM	-0.345	7	0.87	0.974
CMIL-88-NH_2@PCM	-0.345	7	1.26	0.986
CMIL-101-NH_2@PCM	-0.345	7	0.74	0.993
CMIL-100@PCM10	-0.345	7	2.12	0.985
CMIL-100@PCM25	-0.345	7	3.36	0.970
CMIL-100@PCM50	-0.345	7	2.96	0.988
CMIL-100@PCM75	-0.345	7	2.49	0.986
CMIL-100@PCM	-0.345	4	1.63	0.989
CMIL-100@PCM	-0.345	10	1.42	0.982

Table S3. BET surface area of the materials synthesized in this study.

Sample name	BET surface area (m^2/g)
CMIL-88	287.89
CMIL-88-NH_2	217.88
CMIL-100	340.92
CMIL-101	361.56
CMIL-101-NH_2	211.85
PCM	594.76
CMIL-88@PCM	316.55
CMIL-88-NH_2@PCM	230.44

Table S4. Representative kinetic data for electro-Fenton degradation of napropamide (C_0 = 10 ppm).

Sample name	Reaction conditions		k_{SA} (h^{-1} m^{-2} g)
	potential (V)	electrolyte pH	
CMIL-88@PCM	-0.345	7	3.44×10^{-3}
CMIL-100@PCM	-0.345	7	4.99×10^{-3}
CMIL-101@PCM	-0.345	7	2.41×10^{-3}
CMIL-88-NH_2@PCM	-0.345	7	5.78×10^{-3}
CMIL-101-NH_2@PCM	-0.345	7	3.49×10^{-3}

Table S5. Composition of simulated river water (pH 7.0)[1].

Salts	NaCl	KH_2PO_4	$NaNO_3$	Na_2SO_4
Concentration (mg/L)	38.5	1.1	39.4	53.2

Figure S1. Schematic representation of the 3-electrode electrochemical reactor employed in this study.

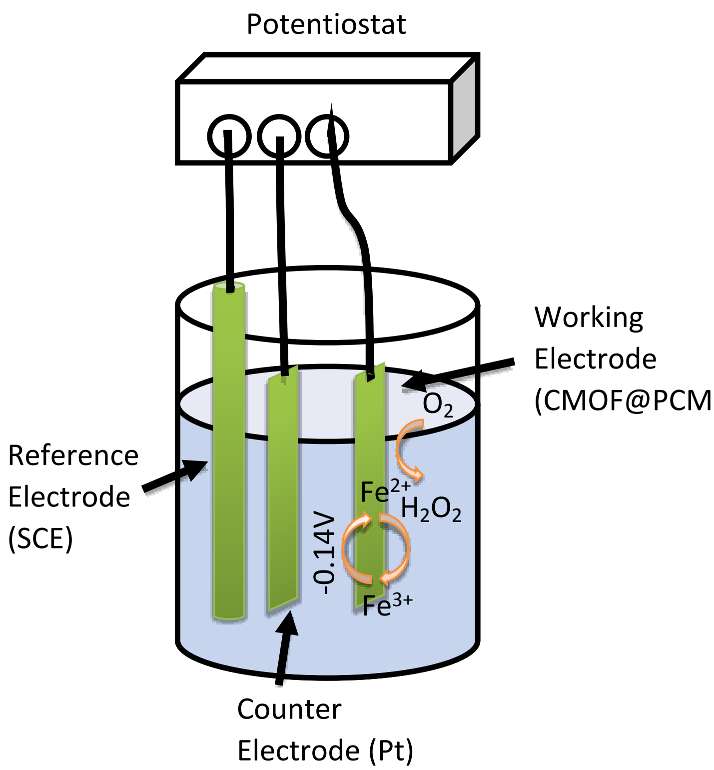

Figure S2. SEM images of MIL-88(Fe) synthesized with (a) 10 mins, (b) 15 mins, (c) 40 mins of microwave irradiations.

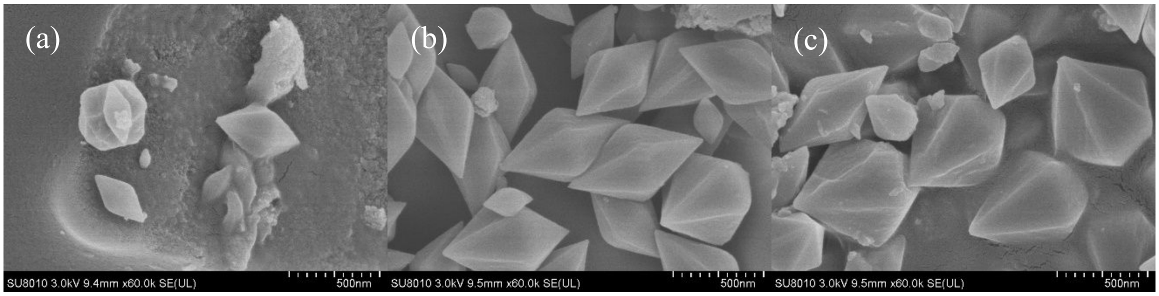

Figure S3. PXRD spectrum of MOFs synthesized by the current study.

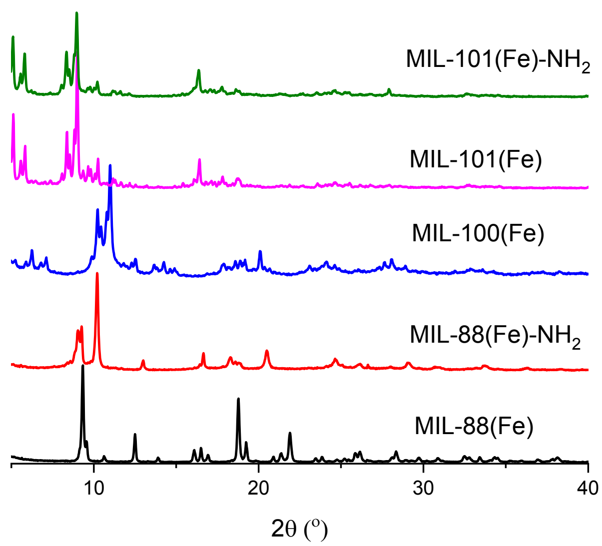

Figure S4. SEM micrographs of (a) CMIL-88, (b) CMIL-100, and (c) CMIL-101.

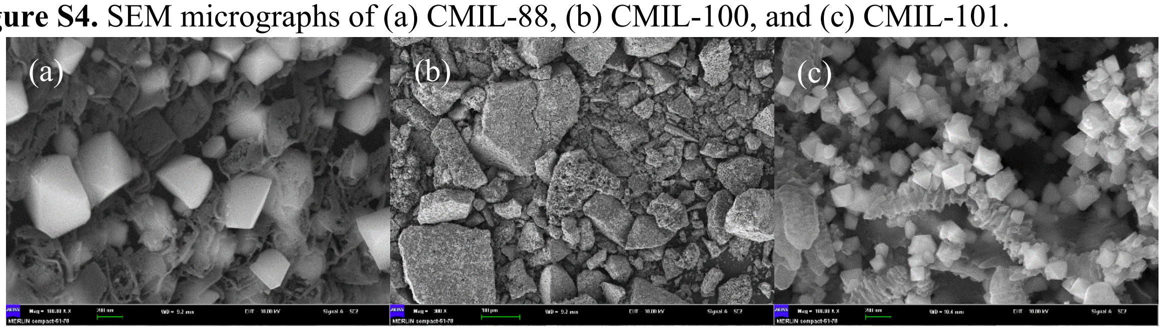

Figure S5. Elemental mapping of (a) CMIL-88, (b) CMIL-100, and (c) CMIL-101.

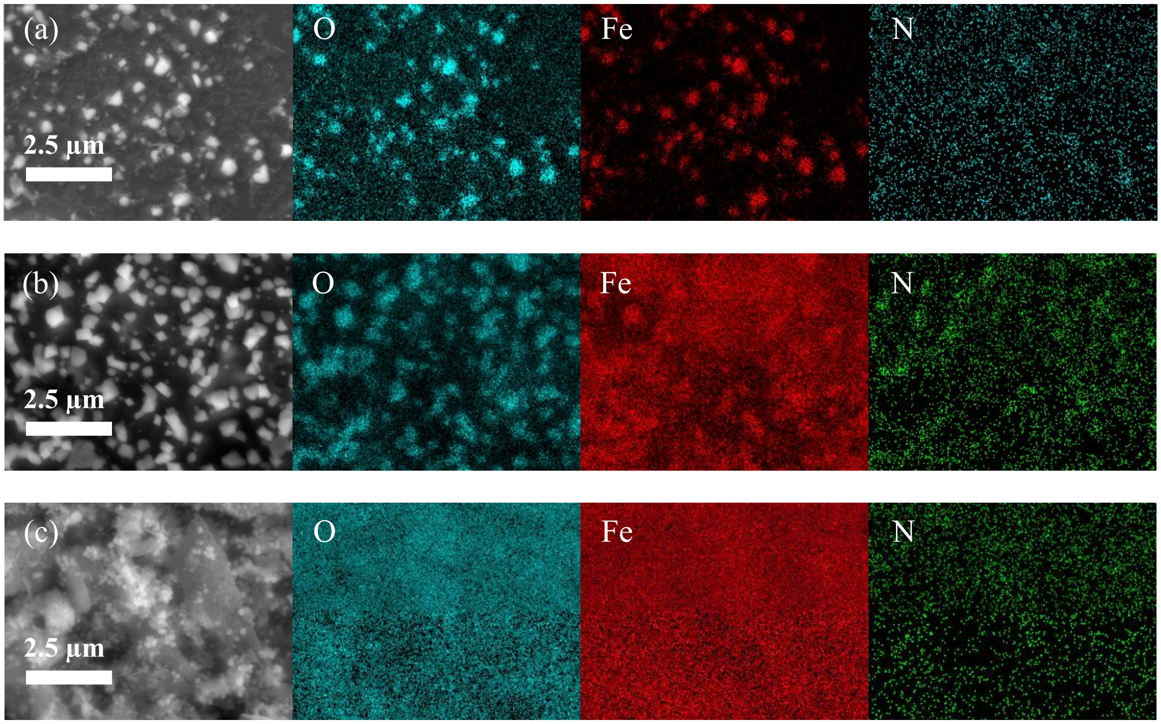

Figure S6. FT-IR spectra of MIL-88(Fe)-NH_2 (left) and CMIL-88-NH_2 (right).

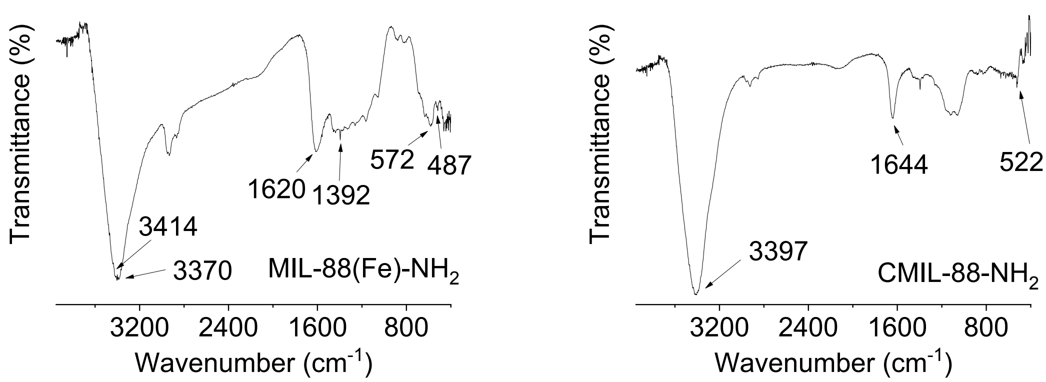

Figure S7. FT-IR spectra of MIL-101(Fe)-NH_2 (left) and CMIL-101-NH_2 (right).

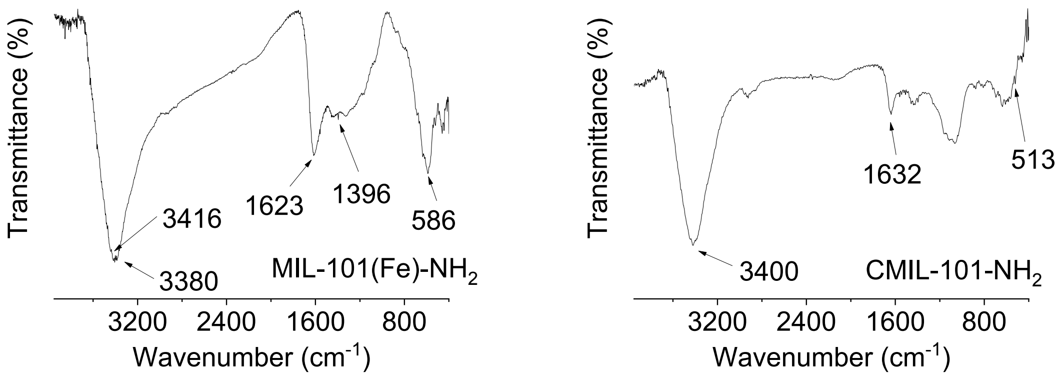

Figure S8. SEM micrograph of CMIL-101 nanoparticles anchored inside the macropore of CMIL-101@PCM.

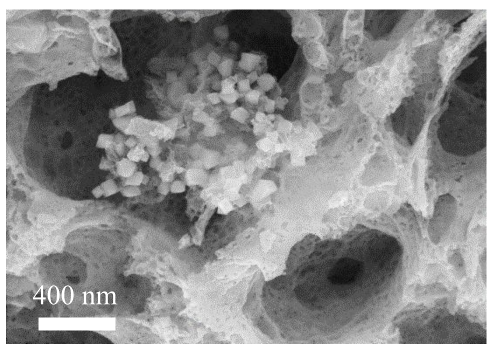

Figure S9. CV curves of PCM substrate in O_2 (black) and Ar (red) saturated electrolyte- solution (0.1 M Na_2SO_4) at (a) pH 4, (b) pH 7, (c) pH 10 with a scan rate of 10 mV/s.

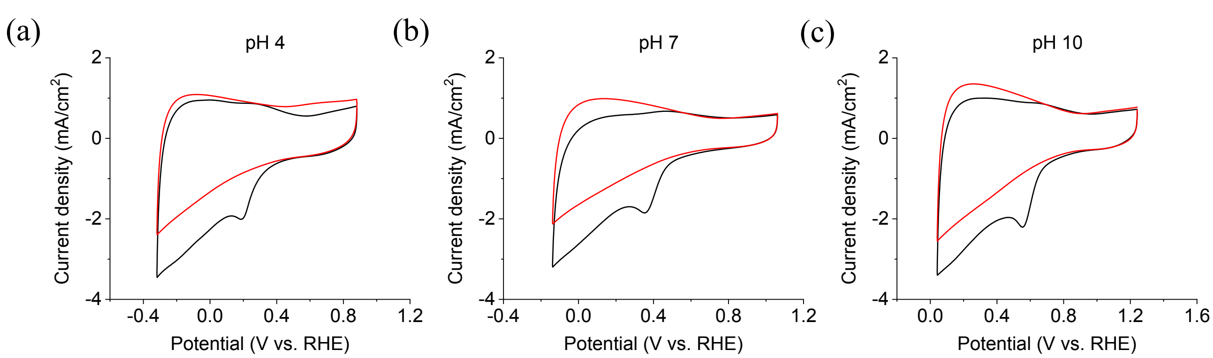

Figure S10. Kinetics of napropamide removal by electro-Fenton using CMOFs@PCM prepared from MIL-88(Fe), MIL-100(Fe), and MIL-101(Fe) (0.1 M Na_2SO_4, pH 7, -0.14V).

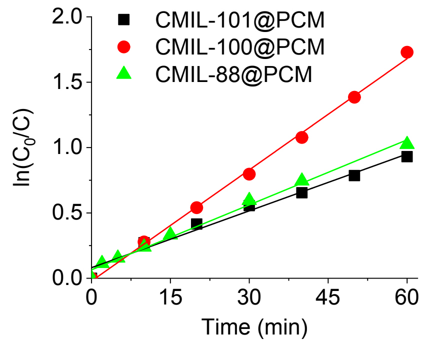

Figure S11. Kinetics of napropamide removal by electro-Fenton using CMOFs@PCM and CMOFs-NH_2@PCM (0.1 M Na_2SO_4, pH 7, -0.14V).

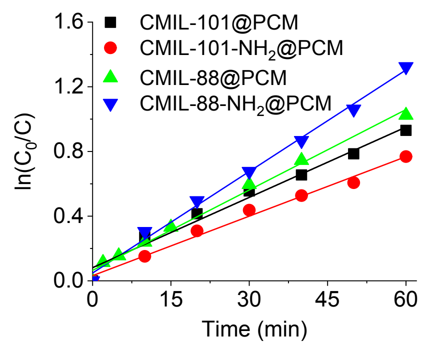

Figure S12. Napropamide removal by electro-Fenton using CMOFs@PCM and CMOFs-NH_2@PCM (0.1 M Na_2SO_4, pH 7, -0.14V).

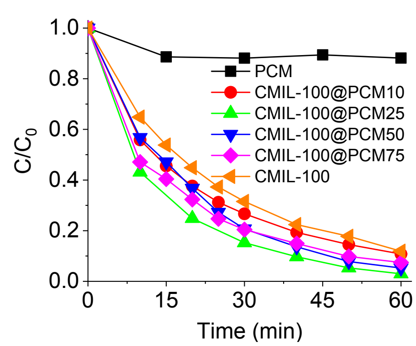

Figure S13. Kinetics of napropamide removal by electro-Fenton using CMOFs@PCM with different doping concentration of CMOFs (0.1 M Na_2SO_4, pH 7, -0.14V).

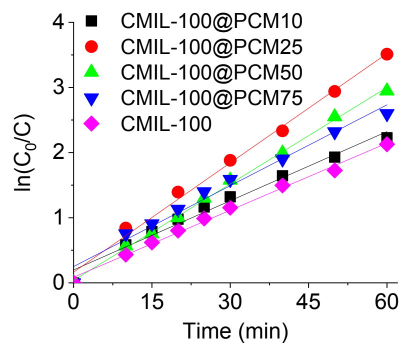

Figure S14. pH effects on napropamide removal efficiency by electro-Fenton using CMIL-100@PCM (0.1 M Na_2SO_4, -0.14V).

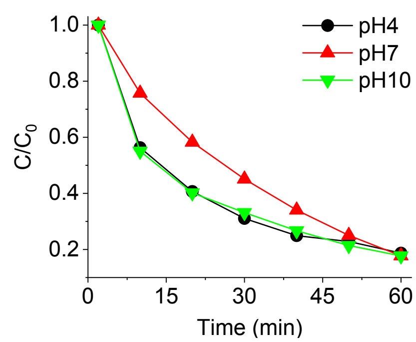

Figure S15. pH effects on napropamide removal kinetics by electro-Fenton using CMIL-100@PCM (0.1 M Na_2SO_4, -0.14V).

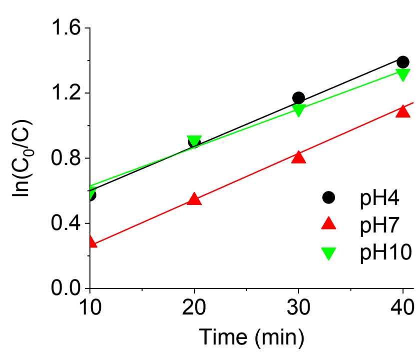

Figure S16. Electrolyte concentration effects on napropamide removal efficiency by electro-Fenton using CMIL-100@PCM (-0.14V).

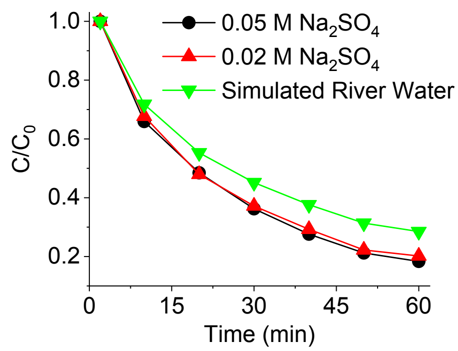

Figure S17. Kinetics of pesticides removal by electro-Fenton using CMIL-100@PCM (0.1 M Na_2SO_4, pH 7, -0.14V).

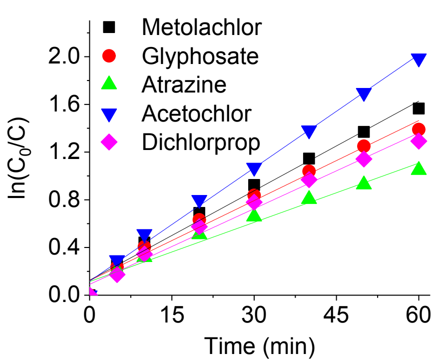

Figure S18. Main reactions involved in the CMOFs@PCM catalyzed electro-Fenton degradation of organic chemical contaminants (Ar denotes aromatic compounds).

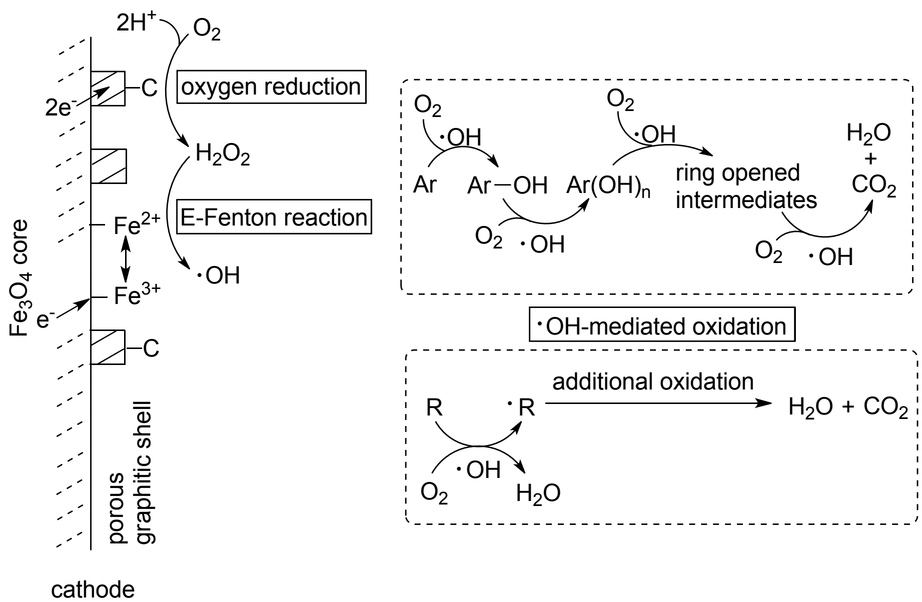

Figure S19. Napropamide degradation efficiency of recycled CMIL-100@PCM electro-Fenton catalyst (0.1 M Na_2SO_4, pH 7, -0.14V).

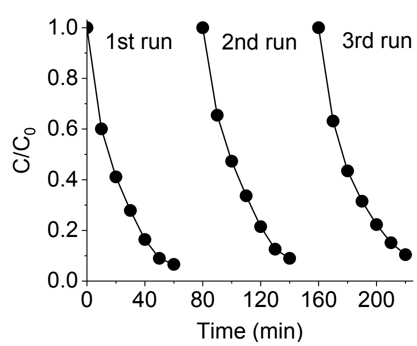

Figure S20. Fe leaching of CMIL-100@PCM and Fe_3O_4@PCM during the electro-Fenton reaction (0.1 M Na_2SO_4, pH 7, -0.14V).

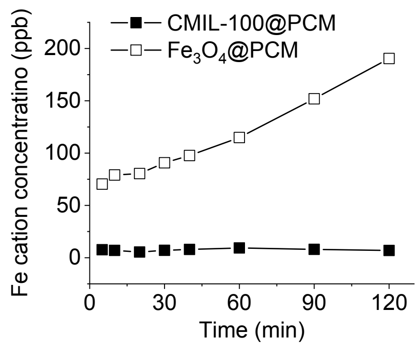

Figure S21. BET surface area analysis of CMIL-88, CMIL-100, and CMIL-101.

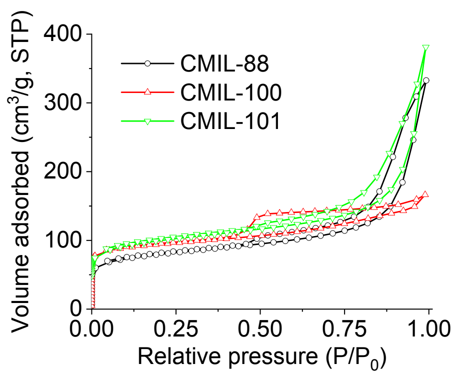

Figure S22. Pore size distribution of CMIL-88, CMIL-100, and CMIL-101.

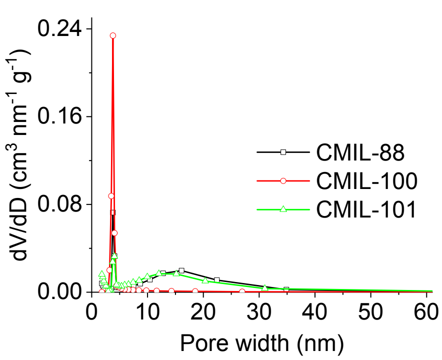

Figure S23. BET surface area analysis of CMIL-88, CMIL-88-NH_2, CMIL-101, and CMIL-101-NH_2.

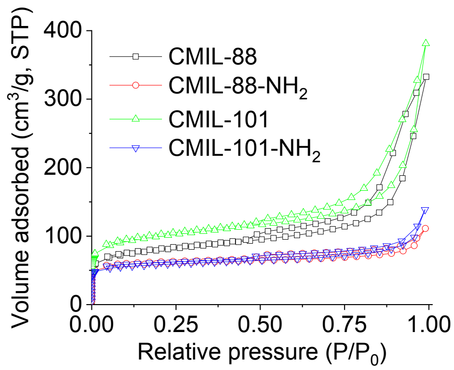

Figure S24. Pore size distribution of CMIL-88, CMIL-88-NH_2, CMIL-101, and CMIL-101-NH_2.

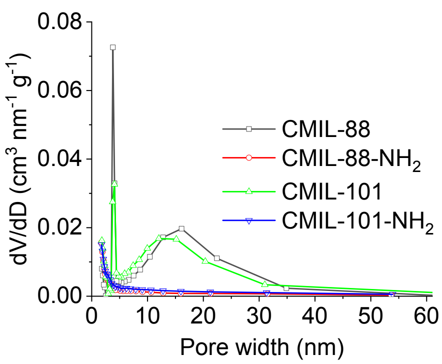

Figure S25. Structure of MIL-88(Fe)-NH_2. Amine functional groups are marked as blue spheres.

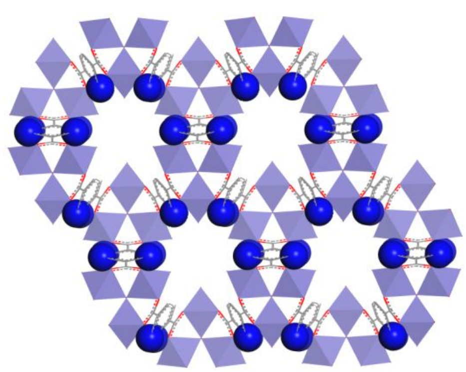

Figure S26. BET surface area analysis of PCM, CMIL-88@PCM, and CMIL-88-NH_2@PCM.

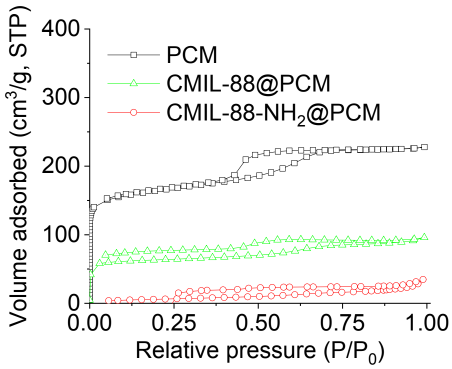

Figure S27. PXRD spectrum of CMOFs synthesized by the current study.

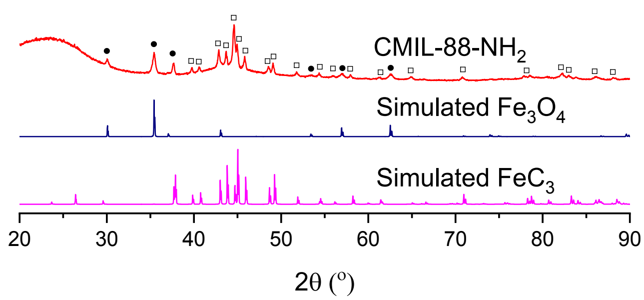

Figure S28. (a) TEM images of CMIL-88@PCM and (b) high-resolution TEM image of magnetite nanoparticles embedded in CMIL-88@PCM.

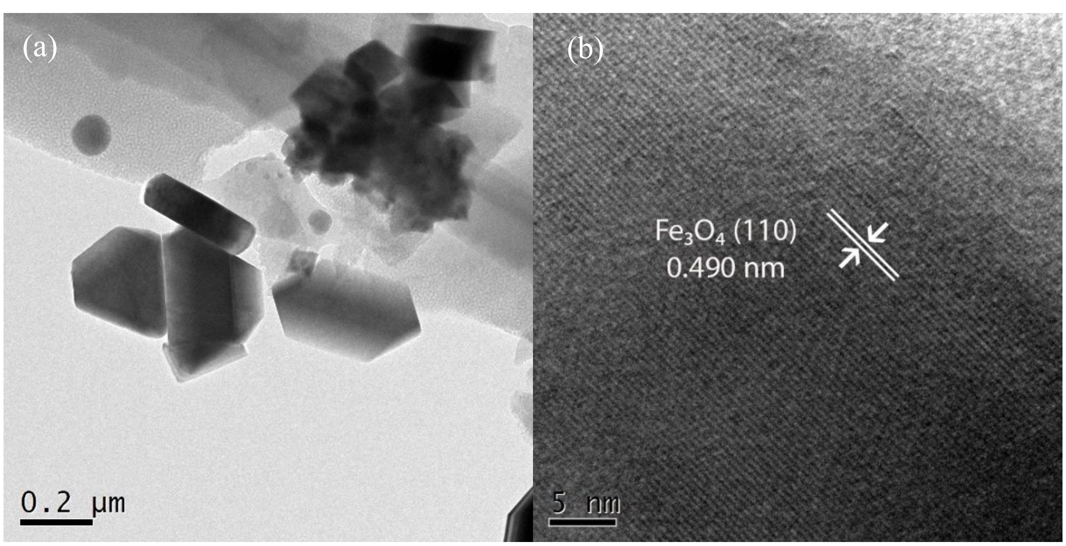

Figure S29. Crystal structure of (a) Fe_3O_4 and (b) Fe_3C unit cell.

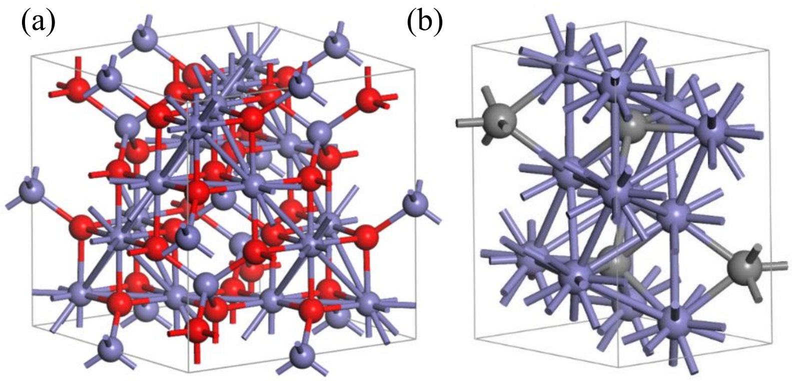

Literatures Cited

(1) Ulberth, F., Certified reference materials for inorganic and organic contaminants in environmental matrices. *Analytical and Bioanalytical Chemistry* **2006,** *386*, (4), 1121-1136.